



Study of the chemical chelates and anti-microbial effect of some metal ions in nanostructural form on the efficiency of antibiotic therapy “norfloxacin drug”

Moamen S. Refat^{a,b,*}, W.F. El-Hawary^{a,c}, Mahmoud A. Mohamed^{a,d}

^a Department of Chemistry, Faculty of Science, Taif University, 888 Taif, Saudi Arabia

^b Department of Chemistry, Faculty of Science, Port Said University, Port Said, Egypt

^c Department of Chemistry, Faculty of Science, Cairo University, Egypt

^d Department of Biochemistry, Faculty of Agriculture, Cairo University, Egypt

ARTICLE INFO

Article history:

Received 29 September 2011

Received in revised form 7 December 2011

Accepted 7 December 2011

Available online 29 December 2011

Keywords:

Norfloxacin
Nano-particles
Lanthanide(III) metals
Anti-microbial
Biological evaluation

ABSTRACT

This paper has reviewed the chemical and biological impact resulting from the interaction between norfloxacin (norH) antibiotic drug and two lanthanide (lanthanum(III) and cerium(III)) metal ions, which prepared in normal and nano-features. La(III) and Ce(III) complexes were synthesized with chemical formulas $[La(nor)_3] \cdot 3H_2O$ and $[Ce(nor)_3] \cdot 2H_2O$. Lanthanum and cerium(III) ions coordinated toward norH with a hexadentate geometry. The norH acts as deprotonated bidentate ligand through the oxygen atom of carbonyl group and the oxygen atom of carboxylic group. Elemental analysis, FT-IR spectral, electrical conductivity, thermal analysis (TG/DTA), X-ray powder diffraction (XRD) and scanning electron microscopy (SEM) measurements have been used to characterize the mentioned isolated complexes. The Coats-Redfern and Horowitz-Metzger integral methods are used to estimate the kinetic parameters for the major successive steps detectable in the TG curve. The brightness side in this study is to take advantage for the preparation and characterization of single phases of La_2O_3 and CeO_2 nanoparticles using urea as precursors via a solid-state decomposition procedure. The norH ligand in comparison with both cases (normal and nano-particles) of lanthanide complexes were screened against antibacterial (*Escherichia Coli*, *Staphylococcus Aureus*, *Bacillus subtilis* and *Pseudomonas aeruginosa*) and antifungal (*Aspergillus Flavus* and *Candida Albicans*) activities. The highest antibacterial and antifungal activities data of the nano-particles complexes were observed with more potent than the free norH and normal lanthanide complexes.

© 2011 Elsevier B.V. All rights reserved.

1. Introduction

Antibiotics can interact with a variety of biomolecules, which may result in inhibition of the biochemical or biophysical processes associated with the biomolecules. This can be illustrated in the interaction of the peptide antibiotic polymyxin with glycolipids which affects membrane function [1].

The intercalation of the anthracyclines (ACs) into DNA base pairs which stops gene replication [2] in the imbedding of the lipophilic antibiotic gramicidin [3] and the insertion of the amphiphilic antibiotic protein into cell membrane [4] which disturb normal ion transport and trans-membrane potential of cells, in the inhibition of transpeptidase by penicillin which affects cell wall synthesis [5] and the inhibition of aminopeptidase by bestatin, amastatin, and puromycin which impairs many significant biochemical processes [6,7].

There are several families of antibiotics that require metal ions to function properly [2–7]. In some cases, metal ions are bound tightly and are integral parts of the structure and function of the antibiotics. Removal of the metal ions thus results in deactivation and/or change in structure of these antibiotics, such as bacitracin, bleomycin (BLM), streptonigrin (SN), and albomycin. In other cases, the binding of metal ions to the antibiotic molecules may engender profound chemical and biochemical consequence, which may not significantly affect the structure of the drugs, such as tetracyclines (TCs), ACs, aureolic acids, and quinolones.

When dealing with the interaction between drugs and metal ions in living systems, a particular attention has been paid to the interaction of metal ions with antibiotics. Antibiotics that interact with metal ions constituted a class of drugs which has been widely used in medicine both for human beings and animals [8,9]. In particular, the interaction between transition metals and β -lactamic antibiotics such as cephalexin had been recently investigated by several physicochemical and spectroscopic methods, and with detailed biological data [10–13]. Many drugs possess modified pharmacological and toxicological properties when

* Corresponding author at: Department of Chemistry, Faculty of Science, Taif University, 888 Taif, Saudi Arabia. Tel.: +966561926288.

E-mail address: msrefat@yahoo.com (M.S. Refat).

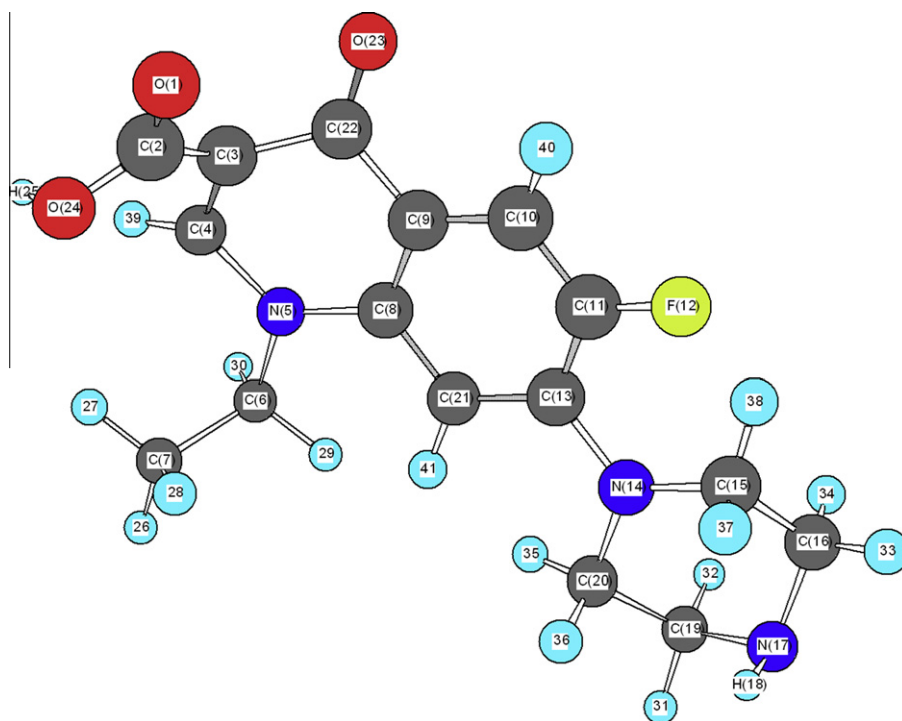


Fig. 1. The structural formula of norH antibiotic drug.

administered in the form of metallic complexes. Probably the most widely studied cation in this respect is Cu(II), for which a host of low-molecular-weight Cu(II) complexes have been proved beneficial against several diseases such as tuberculosis, rheumatoid arthritis, gastric ulcers, and cancers [14–17]. There has been a tremendous growth in the study of drugs from quinolone family, which began with the discovery of nalidixic acid some over 40 years ago. Since then, the exponential growth of this family had produced more than ten thousand analogues [18]. Norfloxacin is considered the best of the third generation quinolone family. There are several reports regarding the synthesis and crystal structure of metal complexes with quinolone derivatives [19–22]. Quinolone antibiotics could participate in the formation of complexes in a number of ways [23–27]. When in acidic media, quinolones are usually singly and/or doubly protonated making them unable to coordinate to the metal cations and, in such cases, only electrostatic interaction are observed between the drug and the metal ions [27,28].

Similar to the case of “metalloproteins,” these antibiotics are dubbed “metalloantibiotics” which are the title subjects of this study. Metalloantibiotics can interact with several different kinds of biomolecules, including DNA, RNA, proteins, receptors, and lipids, rendering their unique and specific bioactivities. In addition to the microbial-originated metalloantibiotics, many metalloantibiotic derivatives and metal complexes of synthetic ligands also show antibacterial, antiviral, and anti-neoplastic activities which are also briefly discussed to provide a broad sense of the term “metalloantibiotics”. There are several metal–norH complexes and their biological activities studies have been reported [23–28], although, the literature survey failed to have any information about the comparison between biological activities of metal ions in nanoparticles coordinated with norH ligand and the normal norH complexes towards metal salts. So interested in this paper is developing a modular form of the effectiveness of antibiotics on the biological effects resulting from the interaction between the lanthanum and cerium ions in nano-structural fashion and norH antibiotic ligand.

2. Experimental

2.1. Reagents

Urea, $\text{CeCl}_3 \cdot 7\text{H}_2\text{O}$, $\text{LaCl}_3 \cdot 6\text{H}_2\text{O}$ and methanol solvent were obtained from Aldrich Company. Norfloxacin drug (Fig. 1) was received from Fluka chemical company. All chemicals used in this study were of analytically reagent grade and used without further purification.

2.2. Synthesis of Ce(III) and La(III)–nor complexes

2.2.1. A normal preparation method

In usual experiment 3 mmol of norH suspended in 30 mL of methanol was mixed with another solution containing 1 mmol of the $\text{CeCl}_3 \cdot 7\text{H}_2\text{O}$ or $\text{LaCl}_3 \cdot 6\text{H}_2\text{O}$ in 10 mL distilled water. The reaction mixture was then basified by adding ammonia solution (5%, V/V) and was kept at 80–90 °C for about 4–5 h. The reaction mixture was maintained basic by adding ammonia solution from time to time. The product obtained as a precipitate was collected by filtration and washed with a mixture of methanol/water (50:50). The product thus obtained was dried (90 °C) under vacuum over anhydrous calcium chloride.

2.2.2. Method of nano-particles preparation

Preparation is in four steps they can be summarized as follows with sequence equations:

- $\text{MCl}_3 \cdot x\text{H}_2\text{O} + \text{Urea} \xrightarrow{\text{ca. } 80^\circ\text{C}} \text{Ln}_2(\text{CO}_3)_3 \cdot x\text{H}_2\text{O}$ (first step) [29,30] (where M = Ce(III) or La(III)).
- $\text{M}_2(\text{CO}_3)_3 \cdot x\text{H}_2\text{O} \xrightarrow{\text{ca. } 800^\circ\text{C}} \text{CeO}_2/\text{La}_2\text{O}_3$ (second step).
- $\text{CeO}_2/\text{La}_2\text{O}_3 + \text{HCl (conc.)} \xrightarrow{\text{ca. } 80^\circ\text{C}} \text{CeCl}_3/\text{LaCl}_3$ (third step).
- $\text{LnCl}_3 + \text{norH} \rightarrow [\text{Ln}(\text{nor})_3] \cdot x\text{H}_2\text{O}$.

The first step of preparation was discussed previously [29,30] as follows: $\text{Ln}_2(\text{CO}_3)_3 \cdot 6\text{H}_2\text{O}$ (Ln=La and Ce) were prepared by mixing aqueous solutions (100 mL) of 0.01 M of the respectively

Table 1
Elemental analysis, molar conductance and melting points data of the La(III) and Ce(III)–nor complexes.

Complexes formula (Mwt)	(Calcd) Found				Molar conductance ($\Omega^{-1} \text{cm}^2 \text{mol}^{-1}$)	Melting point ($^{\circ}\text{C}$)
	%C	%H	%N	%M		
[La(nor) ₃].3H ₂ O (1147.90)	(50.18) 50.09	(4.96) 4.87	(10.98) 10.67	(12.10) 11.95	12	>200
[Ce(nor) ₃].2H ₂ O (1131.11)	(50.92) 50.44	(4.86) 4.76	(11.14) 11.04	(12.39) 12.31	14	>200

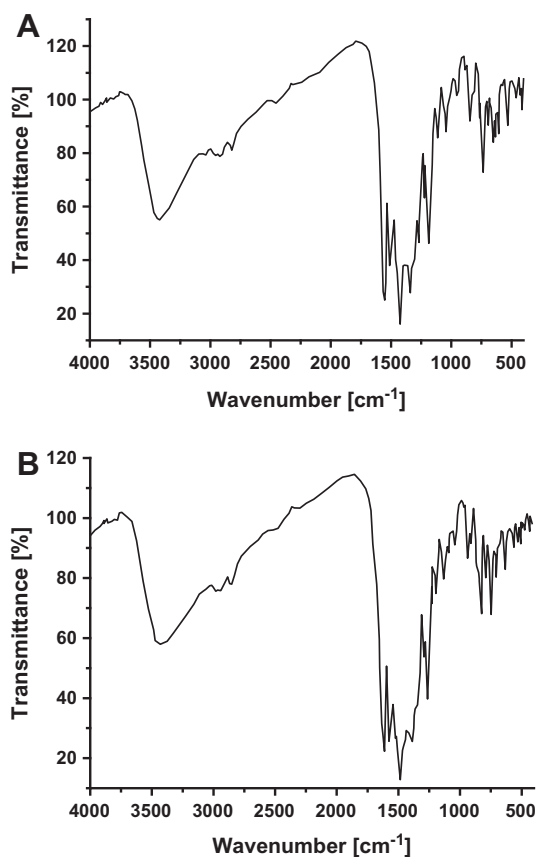


Fig. 2. Infrared spectra of La(III) and Ce(III)–nor complex [A and B, respectively].

Table 2
Main IR peaks of norfloxacin and its complexes.

Compound	$\nu(\text{NH})$	$\nu(\text{C}=\text{O})$	$\nu(\text{COO})$ (asym)	$\nu(\text{COO})$ (sym.)	$\Delta \nu(\text{asym.}-\text{sym.})$	$\nu(\text{M}-\text{O})$
norH	3399	1727	1620	–	–	–
[La(nor) ₃].3H ₂ O	3433	1617	1572	1335	237	506
[Ce(nor) ₃].2H ₂ O	3430	1616	1570	1383	187	506

$\text{LnX}_3 \cdot n\text{H}_2\text{O}$ ($\text{X} = \text{Cl}$; $n = 6$ for La(III) or 7 for Ce(III)) with a volume of 100 mL of 0.1 M of urea. The mixtures were heated to ca. 80 $^{\circ}\text{C}$ for 2–4 h in a water bath. The precipitated white compounds were filtered out, washed several times with hot water, dried at ca. 80 $^{\circ}\text{C}$ in an oven for 2 h and then *in vacuo* over silica gel. Carbonate contents in $\text{Ln}_2(\text{CO}_3)_3 \cdot n\text{H}_2\text{O}$ were determined by dissolving a weighted sample of the products in excess standard HCl and the excess of HCl was determined by titration with standard sodium carbonate. Lanthanide metal La(III) was determined gravimetrically as sesquioxides, Ln_2O_3 , while cerium was determined as CeO_2 . The infrared spectra of urea and lanthanide carbonates were recorded in KBr disks. At room temperature, lanthanide (La and Ce(III)) ions react with urea to form the complex, $\text{Ln}(\text{urea})_3\text{X}_3$ [31–34]. At high temperature, the following reactions may take place:

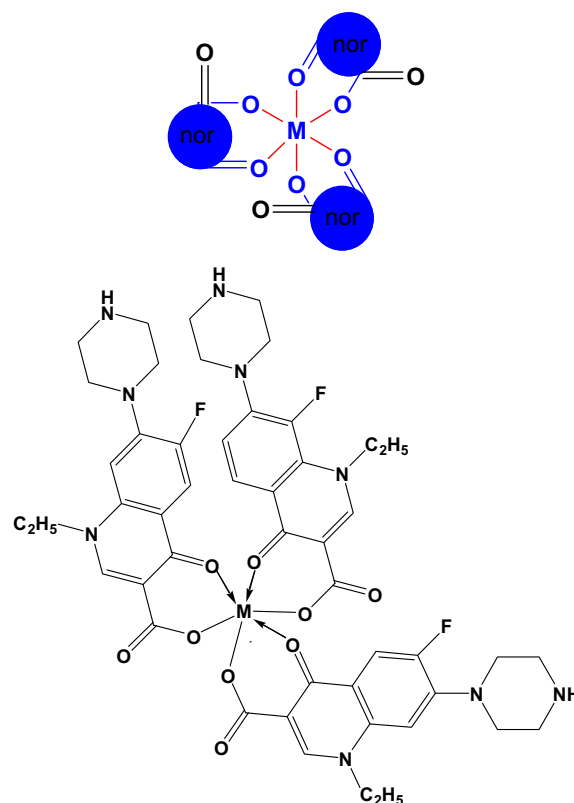
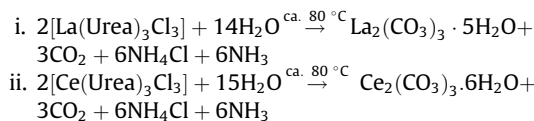


Fig. 3. Suggestion structure of $[\text{M}(\text{nor})_3] \cdot x\text{H}_2\text{O}$ complex (where, $\text{M} = \text{La}$ or $\text{Ce}(\text{III})$).



The second step dealing the transfer of lanthanide(III) carbonates (cerium and lanthanum(III)) constructed in the first step to form of nano-oxides particles, which have been examined using X-ray. In third step lanthanum oxide (Ce(III) and La(III)) was converted to its chloride by treating with concentrated hydrochloric acid. An aqueous solution of lanthanum chloride in fourth step was added to a mixed methanolic solution of norH (the mole ratio $(\text{LnCl}_3 \cdot x\text{H}_2\text{O}) : (\text{norH})$ was 1:3), the pH value of which was adjusted to 8.0–9.0 by adding aqueous ammonia solution (5%, V/V) with heating at 80–90 $^{\circ}\text{C}$ for about 4–5 h and continuous stirring. The precipitate was filtered off, washed with water and methanol, dried (90 $^{\circ}\text{C}$), and then left over anhydrous calcium chloride.

2.3. Equipments

Elemental analyses of carbon, hydrogen and nitrogen elements were analyzed by a Perkin–Elmer CHN 2400 elemental analyzer. The metal contents were determined gravimetrically by converting the compounds to their corresponding oxides. The molar

Table 3
Thermogravimetric data of La(III) and Ce(III)–norH complexes.

Complexes	Steps	DTA peaks (°C) endo (↓), exo (↑)	Decomposed assignments	Weight loss found (calcd.%)
[La(nor) ₃].3H ₂ O	1st, 2nd, 3rd Residue	60 °C (↓) 237 (↓), 486 (↑)	–2H ₂ O·H ₂ O + Dec. nor (C ₁₆ H ₅₁ F ₃ N ₉ O _{7.5}) –	2.27(3.14) 49.88(49.11) ½La ₂ O ₃ + few carbon atoms
[Ce(nor) ₃].2H ₂ O	1st, 2nd, 3rd, 4th Residue	55 (↓), 277 (↓), 488 (↓), 872 (↑)	–2H ₂ O Dec. nor (C ₂₅ H ₅₁ F ₃ N ₉ O ₇) –	3.62(3.18) 56.73(57.11) CeO ₂ + few carbon atoms

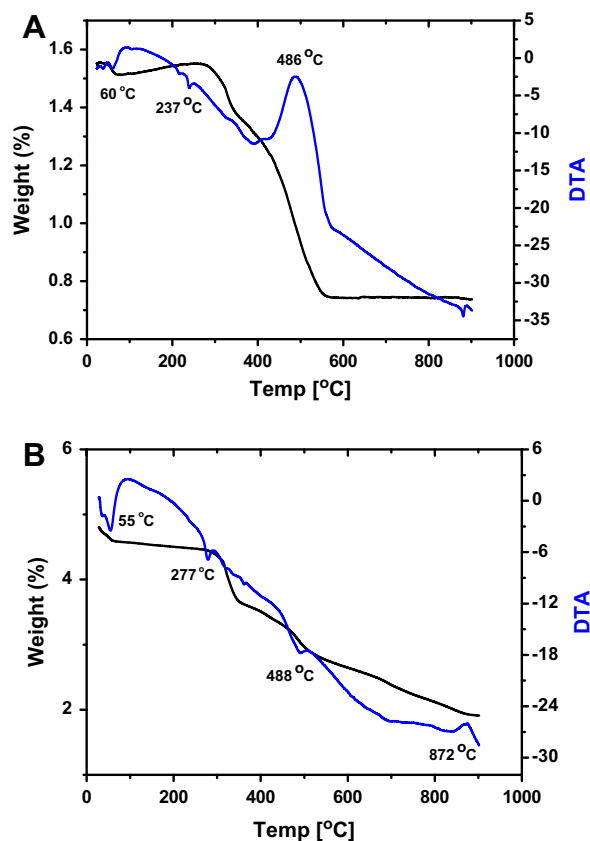


Fig. 4. TG–DTA curves of La(III) and Ce(III)–nor complexes [A and B].

conductivities of freshly prepared 1.0×10^{-3} mol/cm³ dimethylsulfoxide solutions were measured for the soluble complexes using Jenway 4010 conductivity meter. The infrared spectra, as KBr disks, were recorded on a Jasco-4100 FT-IR Spectrophotometer (4000–400 cm⁻¹). The thermal studies were carried out on a Shimadzu thermogravimetric analyzer at a heating rate of 10 °C min⁻¹ under nitrogen till 900 °C. The X-ray diffraction patterns for the two lanthanide oxides (CeO₂ and La₂O₃) were recorded on X'Pert PRO PAN analytical X-ray powder diffraction, target copper with secondary monochromate. Scanning electron microscopy (SEM) images and Energy Dispersive X-ray Detection (EDX) were taken in Joel JSM-6390LA equipment, with an accelerating voltage of 20 KV.

2.4. Biological studies

Anti-microbial activity of the tested samples was determined using a modified Kirby-Bauer disk diffusion method [35]. Briefly, 100 µL of the respective bacteria and fungi were grown in 10 mL of fresh media until they reached account of approximately 10⁸ cells/mL for bacteria or 10⁵ cells/mL for fungi [36]. 100 µL of microbial suspension was spread onto agar plates corresponding to the broth in which they were maintained. Isolated colonies of each organism that might be playing a pathogenic role

should be selected from primary agar plates and tested for susceptibility by disk diffusion method [37,38].

Of the many media available, National Committee for Clinical Laboratory Standards (NCCLS) recommends Mueller-Hinton agar due to: it results in good batch-to-batch reproducibility. Disk diffusion method for filamentous fungi tested by using approved standard method (M38-A) developed by the NCCLS [39] for evaluating the susceptibility of filamentous fungi to antifungal agents. Disk diffusion method for yeast developed standard method (M44-P) by the NCCLS [40]. Plates inoculated with filamentous fungi as *Aspergillus Flavus* at 25 °C for 48 hours; Gram (+) bacteria as *S. Aureus*, *Bacillus subtilis*; Gram (–) bacteria as *Escherichia Coli*, *Pseudomonas aeruginosa* they were incubated at 35–37 °C for 24–48 hours and yeast as *Candida Albicans* incubated at 30 °C for 24–48 h and, then the diameters of the inhibition zones were measured in millimeters [35]. Standard disks of Tetracycline (Antibacterial agent), Amphotericin B (Antifungal agent) served as positive controls for anti-microbial activity but filter disk impregnated with 10 µL of solvent (distilled water, chloroform, DMSO) were used as a negative control.

The agar used is Mueller-Hinton agar that is rigorously tested for composition and pH. Further the depth of the agar in the plate is a factor to be considered in the disk diffusion method. This method is well documented and standard zones of inhibition have been determined for susceptible values. Blank paper disks (Schleicher & Schuell, Spain) with a diameter of 8.0 mm were impregnated 10 µL of tested concentration of the stock solutions. When a filter paper disk impregnated with a tested chemical is placed on agar the chemical will diffuse from the disk into the agar. This diffusion will place the chemical in the agar only around the disk. The solubility of the chemical and its molecular size will determine the size of the area of chemical infiltration around the disk. If an organism is placed on the agar it will not grow in the area around the disk if it is susceptible to the chemical. This area of no growth around the disk is known as a “Zone of inhibition” or “Clear zone”. For the disk diffusion, the zone diameters were measured with slipping calipers of the National for Clinical Laboratory Standards [37]. Agar-based methods such as E-test disk diffusion can be good alternatives because they are simpler and faster than broth methods [41,42].

3. Results and discussion

The two newly complexes of norH with formula [La(nor)₃].3H₂O and [Ce(nor)₃].2H₂O were reported herein and formed from the reaction of the metal(III) chlorides (in normal and nano-size) of La(III) and Ce(III) with the norH drug in 1:3 molar ratio. All of the resulted complexes were stable solids at room temperature (Table 1). Investigation of the solubility of these complexes showed that they were insoluble in methanol, ethanol, diethylether, benzene, chloroform and carbon tetrachloride but soluble in dimethylformamide (DMF) and dimethylsulfoxide (DMSO) with gently heating. Testing for chloride ions held as follows; the solid complexes were acidified by adding few drops of concentrated nitric acid. The nitric acid reacts with, and removes, other ions that might also give a confusing precipitate with silver nitrate. The basis of the

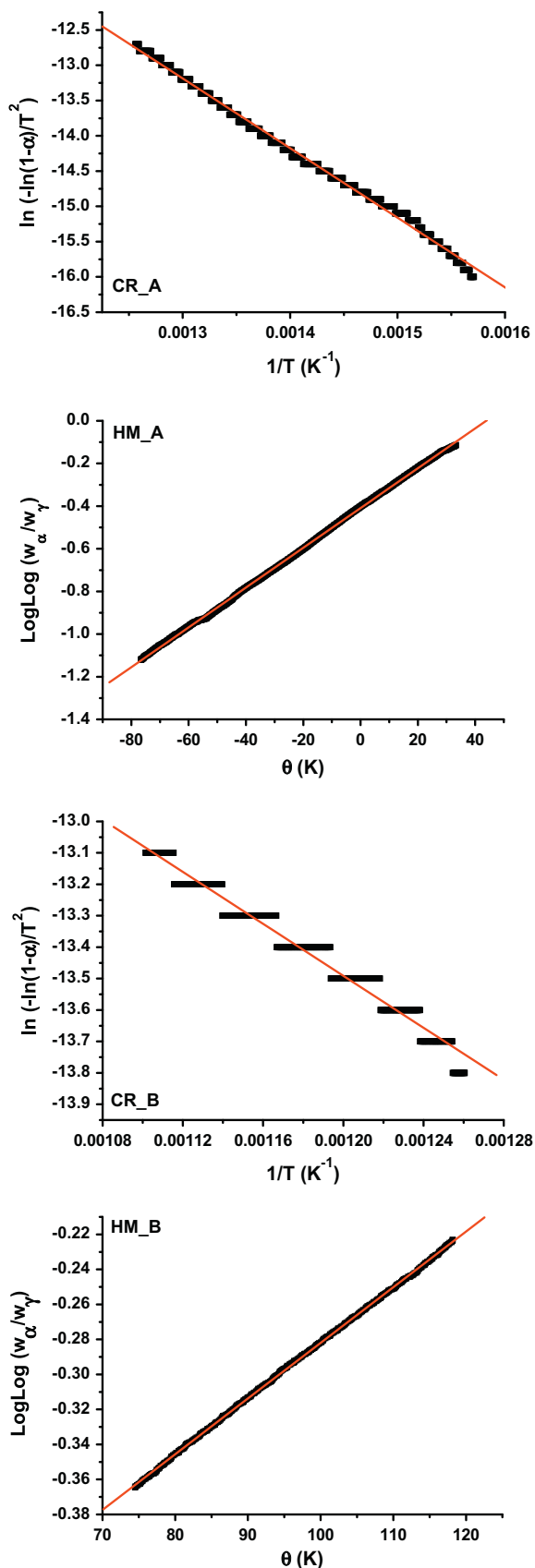


Fig. 5. Plots of Coats–Redfern (CR) and Horowitz–Metzger (HM) relations for La(III) and Ce(III)–nor complexes [A and B].

test is that a solution containing chloride ions changes immediately into a whitish solution when silver nitrate solution is added (0.1 mol/L). If these chloride ions are not present, the solution remains clear and transparent. The molar conductance of the isolated complexes indicated that all the complexes were non-electrolytes [43] which agreed with the elemental analysis data and the absence of chloride ions.

3.1. IR spectral analyses

Based on the comparison between infrared spectra of the prepared La(III) and Ce(III) complexes (Fig. 2) with that of the free norH ligand, the place of coordination of the ligand sharing in the chelating with the metal ions for both norH complexes have been justified and summarized in Table 2. The norH ligand showed strong broad band near at 3400 cm^{-1} . This band could be assigned to the stretching vibration of the $\nu(\text{N}-\text{H})$ group. This band existed in the spectra of the two complexes that indicate the non-participation of this group in the coordination process with metal ions [44]. The free ligand has a two strong bands located at 1620 and 1727 cm^{-1} which assigned to the stretching vibration of the carboxylic $\nu(\text{COOH})$ and the carbonyl $\nu(\text{CO})$ groups [19]. Insight into the spectrum of norH, it was found that the absence of the ν_{COOH} stretching vibration, explains strongly the deprotonation of norH ligand [45]. In the literature survey [19] a study which deals with the location of both asymmetric (1585 cm^{-1}) and symmetric (1380 cm^{-1}) stretching depending upon the deprotonation of carboxylate group. The main infrared spectral bands detectable for the norH ligand in the prepared complexes (Table 2) confirm the deprotonation situation for the norH complexes. In the chelation process, the carbonyl $\nu(\text{CO})$ group was disappeared and the $\nu(\text{COOH})$ stretching vibration in norH ligand appeared at (1617 and 1616 cm^{-1} and (1335 and 1383 cm^{-1} due to the asymmetric and symmetric stretching vibration of the ligated COO^- group, respectively [44,19,45]. From the facts proven that the carboxylate group has three types of coordination (unidentate, bidentate or bridge), then the basis of these knowledge can be said that unidentate chelation take place when the difference in frequencies between asymmetric and symmetric stretching vibrations $[\Delta\nu = (\nu_{\text{asym}}\text{COO}^- - \nu_{\text{sym}}\text{COO}^-)] \geq 200$ [44,19,45]. From the infrared spectra of both La and Ce(III) complexes the calculated $\Delta\nu$ was observed at 237 and 187 cm^{-1} , respectively, which suggests a uni-dentate interaction of the carboxylate group toward the central metal ions in both norH complexes. The other reason, which confirms the place of coordination is that the carbonyl group $\nu(\text{C}=\text{O})$ which presence at 1727 cm^{-1} for the free norH was blue shifted by $\Delta\nu = 110$ and 111 cm^{-1} for La(III) and Ce(III)–norH complexes, respectively. This discussion is strengthen the involvement of the carbonyl group in coordination of La(III) and Ce(III) complexes. The new band was involved in both La(III) and Ce(III) complexes at 506 cm^{-1} assigned to M–O stretching vibration motion [19,45]. The uncoordinated water molecules in the La(III) and Ce(III) complexes were observed at the $\sim 3430\text{ cm}^{-1}$ overlapping with the same place of $\nu(\text{NH})$ band. From the above discussion we can say that, norH ligand coordinated with La(III) and Ce(III) ions via two oxygen atoms of the carboxylate and the carbonyl groups, the most probable six coordinated fashion around each metal ion (Fig. 3) as designed below.

3.2. Thermal analysis

The thermal decomposition process and mechanism of lanthanum and cerium(III) complexes with norH were studied (Fig. 4 and Table 3). On heating in nitrogen atmosphere, the TG–DTA curves of norH complexes show three processes (one dehydration and two decompositions) for lanthanum–nor complex and four processes (one dehydration and three decompositions) for

Table 4
Kinetic parameters using the Coats–Redfern (CR) and Horowitz–Metzger (HM) equations for the La(III) and Ce(III)–nor complexes.

Complex	DTA _{max}	Method	Parameter					r
			E (J mol ⁻¹)	A (s ⁻¹)	ΔS (J mol ⁻¹ K ⁻¹)	ΔH (J mol ⁻¹)	ΔG (J mol ⁻¹)	
La(III)	486	CR	8.21 × 10 ⁴	1.74 × 10 ³	−1.91 × 10 ²	7.58 × 10 ⁴	2.21 × 10 ⁵	0.9979
		HM	10.3 × 10 ⁴	6.52 × 10 ⁴	−1.61 × 10 ²	9.66 × 10 ⁴	2.19 × 10 ⁵	0.9998
Ce(III)	488	CR	3.44 × 10 ⁴	2.04 × 10 ⁻¹	−2.66 × 10 ²	2.81 × 10 ⁴	2.30 × 10 ⁵	0.9859
		HM	3.53 × 10 ⁴	4.83 × 10 ⁻¹	−2.59 × 10 ²	2.89 × 10 ⁴	2.26 × 10 ⁵	0.9998

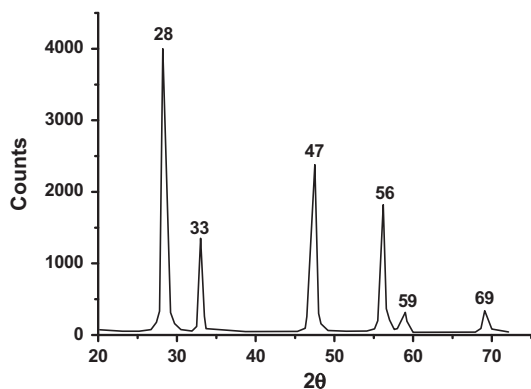


Fig. 6. The XRD spectrum of CeO₂.

Table 5
XRD spectral data of the highest value of intensity of the Ce(III) residual at 600 °C.

Residuals	2θ	FWHM	Relative intensity	Particle size (nm)
CeO ₂	28	0.7125	100	12

cerium–nor complex, the final products are the mixtures of lanthanide oxides and few carbon atoms.

Fig. 4A and B shows the TG–DTA curves of La(nor)₃·3H₂O and Ce(nor)₃·2H₂O in nitrogen environment, respectively. From these Figs, the following results can be discussed. In a nitrogen atmosphere, the TG–DTA curves of the La(III) and Ce(III) hydrated complexes show two mainly and sub steps: one is dehydration process and another is decomposition process. The processes of dehydration are accompanied by endothermic peaks and the

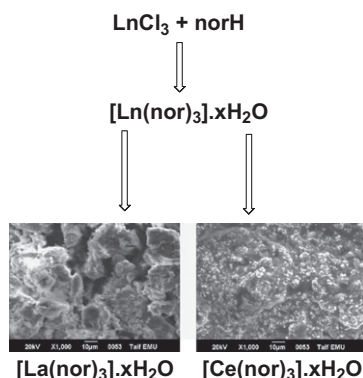


Fig. 7A. SEM images of La(III) and Ce(III)–nor complexes synthetic by conventional method.



Fig. 7B. SEM images of La(III) and Ce(III)–nor complexes synthetic using oxides in nano-sized particles.

decomposition processes are accompanied by weak-to-strong endo and exo-thermic peaks. The final residues of decomposition of the lanthanum and cerium–nor complexes are mixtures of lanthanide oxides (CeO₂ or La₂O₃) and few carbon atoms. The lanthanide oxides (CeO₂ or La₂O₃) and the few carbon atoms were calculated by the combustion method and the content of carbon in the residual products was determined by mass loss after the final mixed products of lanthanide oxides and carbon were combustion in static air. Table 3 shows the TG–DTA data. The result of TG–DTA agreed with that of elemental analysis. Survival of a few number of carbon atoms in the final decomposition step can be interpreted due to the presence of many aromatic rings (three moieties of norH ligand) with a lack of oxygen atoms. The different thermal decomposition process from La(III)–to–Ce(III) complexes because of the lanthanide contraction and difference in the ionic radii of La³⁺ (106.1 pm) and Ce³⁺ (103.4 pm). The three terminal of ethyl groups and fluorine atoms of the three norH moieties are the early groups which vulnerable and lose in the form of ethylene and hydrogen fluoride molecules, respectively. The presence of chelation via three norH towards lanthanide ions is one of the factors causing hinders the coordination of water molecule to sharing in the complexation. The La₂O₃ and CeO₂ oxides are stable in the temperature range 560–900 °C.

Table 6
Selected values of bond lengths and bond angles of La(III) and Ce(III)-complexes.

Complex	Bond length	Bond angle			
La(III)- nor	C(6)–O(8)–La(37)	109.472	O(8)–La(37)–O(9)	89.999	
		C(7)–O(9)–La(37)	109.619	O(8)–La(37)–O(20)	89.999
	C(18)–O(20)–La(37)		109.470	O(8)–La(37)–O(21)	90.000
		C(19)–O(21)–La(37)	109.601	O(8)–La(37)–O(32)	89.999
	C(30)–O(32)–La(37)		109.472	O(9)–La(37)–O(33)	89.999
		C(31)–O(33)–La(37)	109.559	O(9)–La(37)–O(20)	179.451
	Ce(III)- nor		O(8)–Ce(37)	2.290	O(9)–La(37)–O(21)
		O(9)–Ce(37)		2.290	O(9)–La(37)–O(32)
			O(20)–Ce(37)	2.290	O(9)–La(37)–O(33)
		O(21)–Ce(37)		2.290	O(20)–La(37)–O(21)
			O(32)–Ce(37)	2.290	O(20)–La(37)–O(32)
		O(33)–Ce(37)		2.290	O(20)–La(37)–O(33)
			C(6)–O(8)–Ce(37)	109.470	O(21)–La(37)–O(32)
		C(7)–O(9)–Ce(37)		111.699	O(21)–La(37)–O(33)
C(18)–O(20)–Ce(37)			109.470	O(32)–La(37)–O(33)	90.000
		C(19)–O(21)–Ce(37)	111.644		
O(8)–Ce(37)–O(9)			89.999		
		O(8)–Ce(37)–O(20)	89.999		
O(8)–Ce(37)–O(21)			90.000		
		O(8)–Ce(37)–O(32)	89.999		
O(8)–Ce(37)–O(33)	89.999				
	O(9)–Ce(37)–O(20)	179.451			
O(9)–Ce(37)–O(21)		90.572			
	O(9)–Ce(37)–O(32)	90.000			
O(9)–Ce(37)–O(33)		0.000			
	O(20)–Ce(37)–O(21)	90.000			
O(20)–Ce(37)–O(32)		90.572			
	O(20)–Ce(37)–O(33)	179.451			
O(21)–Ce(37)–O(32)		0.547			
	O(21)–Ce(37)–O(33)	90.572			
O(32)–Ce(37)–O(33)		90.000			

3.3. Kinetic data

The thermodynamic parameters of decomposition processes of both La(III) and Ce(III) complexes, called, activation energy (E_a), enthalpy (ΔH^*), entropy (ΔS^*), and Gibbs free energy change of (ΔG^*) were evaluated graphically by employing the Coats–Redfern and Horowitz–Metzger methods [46,47]. These methods are an integral methods assuming various orders of reaction and comparing the linearity in each case to select the correct order by using.

3.3.1. Coats–Redfern equation

$$\ln \left[\frac{1 - (1 - \alpha)^{1-n}}{(1 - n)T^2} \right] = \frac{M}{T} + B \text{ for } n \neq 1 \quad (1)$$

$$\ln \left[\frac{-\ln(1 - \alpha)}{T^2} \right] = \frac{M}{T} + B \text{ for } n = 1 \quad (2)$$

where $M = \psi - E/R$ and $B = \ln AR/\psi E$; each of E , R , A , and ψ are the heat of activation, the universal gas constant, pre-exponential factor and heating rate, respectively. The correlation coefficient, r , was computed using the least square method for different values of n , by plotting the left-hand side of Eqs. (1) and (2) versus $1000/T$ (Fig. 5A and B).

3.3.2. Horowitz–Metzger equation

The relations derived are as follows:

$$\ln[-\ln(1 - \alpha)] = \frac{E}{RT_m} \Theta \quad (3)$$

where α is the fraction of the sample decomposed at time t and $\Theta = T - T_m$.

A plot of $\ln[-\ln(1 - \alpha)]$ against Θ , was found to be linear, from the slope of which E , was calculated and Z can be deduced from the relation:

$$Z = \frac{E\varphi}{RT_m^2} \exp\left(\frac{E}{RT_m}\right) \quad (4)$$

where φ is the linear heating rate, from the intercept and linear slope of such stage, the A (Arrhenius factor) and E_a values were determined. The other kinetic parameters, ΔH , ΔS and ΔG were computed using the relationships:

$$\Delta H = E - RT \quad (5)$$

$$\Delta S = R \ln(Ah/kT) \quad (6)$$

$$\Delta G = \Delta H - T\Delta S \quad (7)$$

where k is the Boltzmann's constant and h is the Planck's constant.

The kinetic data obtained from the non-isothermal decomposition of the complexes are given in Table 4. The activation energy of the complexes is expected to increase with decreasing metal ion radius [48–50]. The smaller size of metal ions permits a closer approach of the ligand. Hence, the ΔE^* value in the main stages for the Ce(III) complex is higher than La(III) complex. The calculated ΔE^* values using Coats–Redfern and Horowitz–Metzger methods for the main decomposition stage of the complexes are found to be $E_a \text{ Ce} = 48.85 \text{ kJ mol}^{-1} > E_a \text{ La} = 92.55 \text{ kJ mol}^{-1}$ which is in accordance with $r\text{Ce(III)} = 103.4 \text{ pm} < r\text{La(III)} = 106.1 \text{ pm}$, this is contrary to reality where it could be interpreted as because of lanthanide contraction phenomena. The negative values of ΔS^* see Table 4, indicate that the reaction rates are slower than normal [51]. Furthermore, these data indicate that the activated complexes have more ordered structure than the reactants.

3.4. XRD and SEM studies

The X-ray powder diffraction patterns (Fig. 6) in the range of $20^\circ < 2\theta < 75^\circ$ for the residual products of burning at 600°C which resulted from the interaction between LaCl_3 or CeCl_3 with urea were carried in order to obtain an idea about the lattice dynamics of the resulted oxides of La(III) and Ce(III). For example the values of 2θ , full width at half maximum (FWHM) of prominent intensity peak, relative intensity and particle size of Ce(III) oxide as a residual product were compiled in Table 5. The crystallite size of the Ce(III) oxide could be estimated from XRD patterns by applying FWHM of the characteristic peaks using Deby–Scherrer Eq. (8) [52]:

$$D = K\lambda/\beta \cos \theta \quad (8)$$

where D is the particle size of the crystal grain, K is a constant (0.94 for Cu grid), λ is the X-ray wavelength (1.5406 Å), θ is the Bragg diffraction angle and β is the integral peak width. The particle size was estimated according to the highest value of intensity compared with the other peaks. The particle size for the Ce(III) thus obtained was 12 nm. These data gave an impression that the particle size located within nanoscale range.

Scanning electron microscopy is a simple tool used to give an impression about the microscopic aspects of the physical behavior of norH drug as a complexing agent and of the complex formation (Figs. 7A and 7B). Although this tool is not a qualified method to confirm complex formation but it can be a reference to the presence of a single component in the synthetic products. The pictures of the La(III) and Ce(III) complex show a small particle size with an nanofeature products.

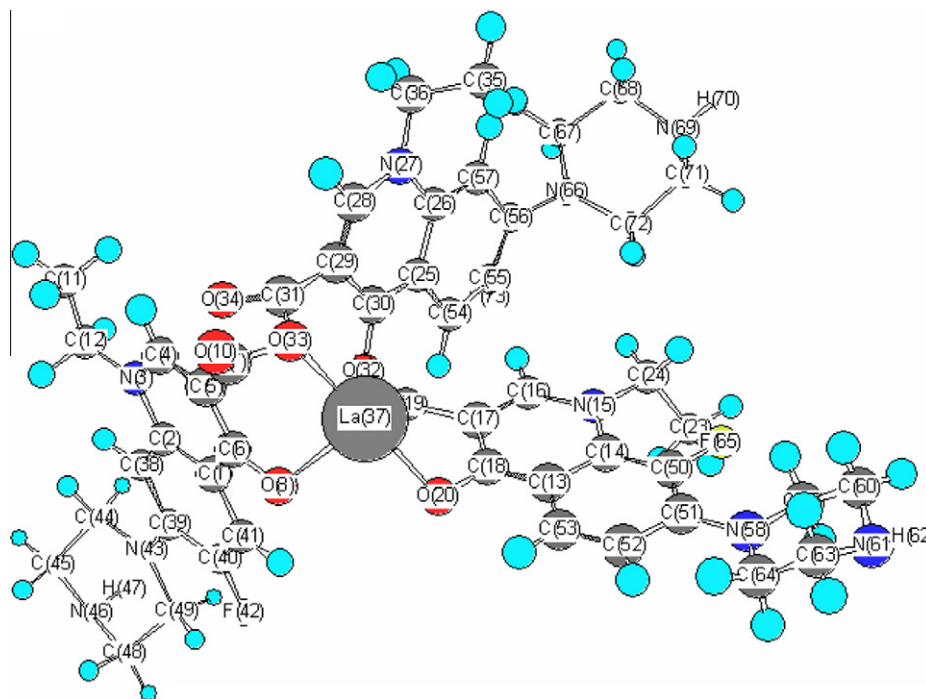


Fig. 8. Optimized structure of La(III)-nor complex.

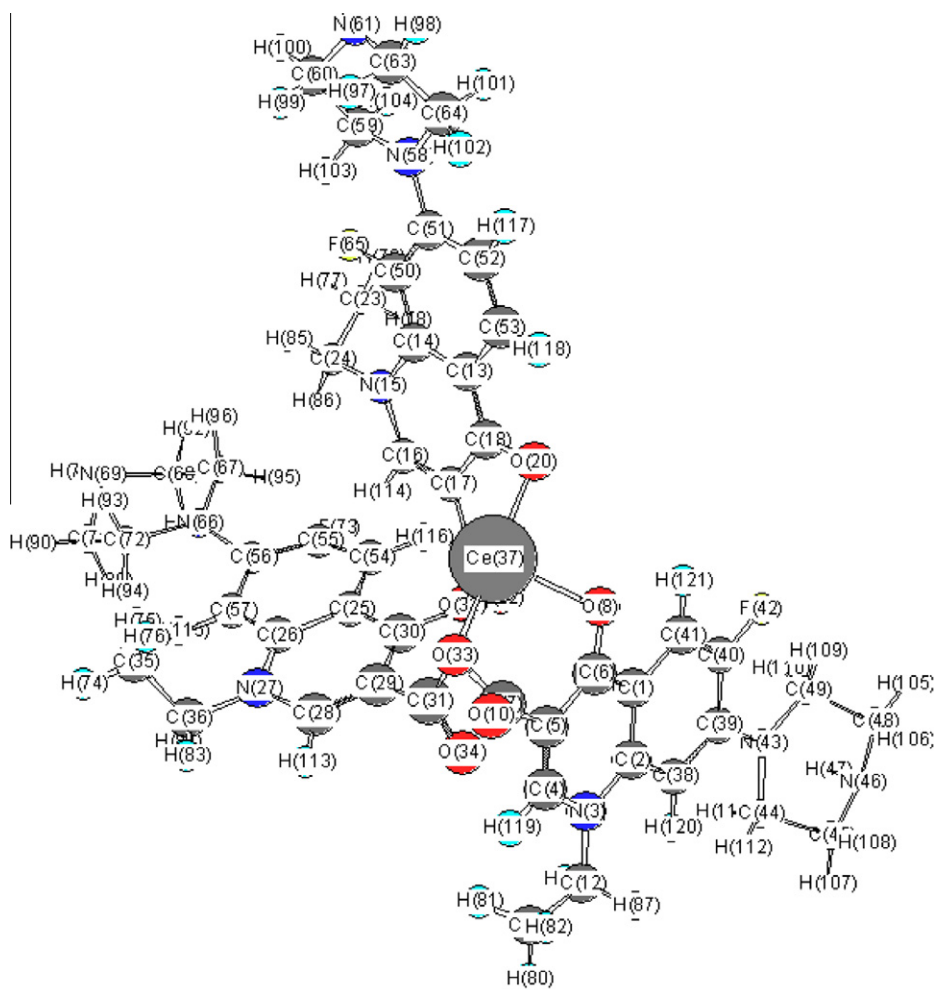


Fig. 8 (continued)

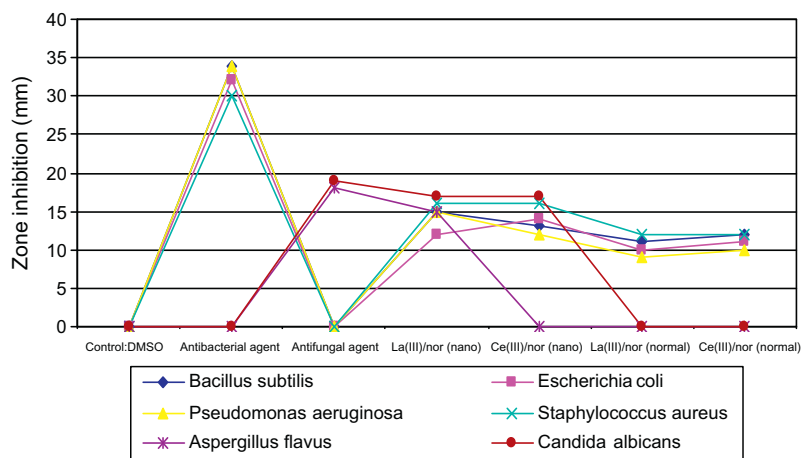


Fig. 9. Optimized structure of Ce(III)–nor complex.

Table 7

Inhibition zone diameter (mm) of the target compounds against tested microorganisms.

Sample	Inhibition zone diameter (mm/mg sample)					
	<i>Bacillus subtilis</i> (G ⁺)	<i>Escherichia coli</i> (G ⁻)	<i>Pseudomonas aeruginosa</i> (G ⁻)	<i>Staphylococcus aureus</i> (G ⁺)	<i>Aspergillus flavus</i> (Fungus)	<i>Candida albicans</i> (Fungus)
Control: DMSO	0.0	0.0	0.0	0.0	0.0	0.0
Distilled water						
<i>Standard</i>						
Antibacterial agent (Tetracycline)	34	32	34	30	-	-
Antifungal agent (Amphotericin B)	-	-	-	-	18	19
La(III)/nor (nano)	15	12	15	16	15	17
Ce(III)/nor (nano)	13	14	12	16	0.0	17
La(III)/nor (normal)	11	10	9	12	0.0	0.0
Ce(III)/nor (normal)	12	11	10	12	0.0	0.0

G: Gram reaction. Solvent: DMSO.

3.5. Molecular modeling of complexes

Molecular modeling had been successfully used to detect three dimensional arrangements of atoms in complexes. The selected bond lengths and bond angles values of the coordinated complexes were summarized and refereed in Table 6. This calculation for La(III) and Ce(III)–nor complexes were obtained by using the commercial available molecular modeling software Chem Office Ultra-7. These statistical data agreed with Figs. 8 and 9 confirmed six coordinated structures of both complexes toward metal ions.

3.6. Biological studies

Biological studies were observed in term anti-microbial activities of target compounds against gram-positive (*B. subtilis* and *S. aureus*) and gram-negative (*E. coli* and *P. aeruginosa*) and tow strains of fungus (*A. flavus* and *C. albicans*). Result from the agar disk diffusion tests for anti-microbial activities of target compounds are presented in Table 7, and illustrated in Fig. 9.

All tested compounds displayed a different degree of anti-microbial effect and compounds in nanotype (La(III)/nor and Ce(III)/nor) displayed a degree of anti-microbial activities greater than same compounds in normal type against all organisms tested except nanotype of Ce(III)/nor with *A. flavus* fungus strain.

Regarding the inhibition zone diameter, La(III)/nor compound in nanotype has highest anti-microbial activity against all target organisms compared to other three tested compounds. Also, La(III)/nor compound in nanotype gained approximately 50% of activity of antibacterial agent (Tetracycline) and Antifungal agent (Amphotericin B). La(III)/nor and Ce(III)/nor compounds in normal types displayed only antibacterial activity with approximately 30% of activity of antibacterial agent (Tetracycline). The remarkable activity of La(III)/nor compound in nanotype may be due to the outer membrane of all target organism (bacteria or fungus) more permeable for La(III)/nor compound in nanotype structure. The most reasons for lethal action of tested compounds may due to their interactions with critical intercellular sites causing the death of cells [52]. The variety of anti-microbial activities of tested compounds may due to a different degree of tested compounds penetration through cell membrane structure of target organism. In conclusion, the interactions between the lanthanum and cerium ions in nano-structural form resulting developing of the effectiveness of biological characters of lanthanum and cerium ions antibiotics.

Acknowledgment

This work was supported by grants from Taif University under Project Grants no. 1030-432-1.

References

- [1] S.A. David, K.A. Balasubramanian, V.I. Mathan, P. Balaram, *Biochim. Biophys. Acta* 1165 (1992) 145.
- [2] (a) J.W. Lown, *Chem. Soc. Rev.* 22 (1993) 65;
(b) D.R. Phillips, C. Cullinane, H. Trist, R.J. White, *In vitro* transcription analysis of the sequence specificity of reversible and irreversible complexes of adriamycin with DNA, in: B. Pullman, J. Jortner (Eds.), *Molecular Basis of Specificity in nucleic acid–drug interactions*, Springer, Berlin, 1990, pp. 137–155.
- [3] J.F. Hinton, R.E. Koeppe, *Biol. Syst.* 19 (1985) 173.
- [4] M.W. Parker, F. Pattus, A.D. Tucher, D. Tsernoglou, *Nature* 337 (1989) 93.
- [5] (a) T. Oka, K. Hashizume, H. Fujita, *J. Antibiot.* 33 (1980) 1357;
(b) J.M. Frere, J.M. Ghuysen, P.E. Reynolds, R. Moreno, *Biochem. J.* 143 (1974) 241.
- [6] (a) H. Umezawa, M. Ishizuka, H. Suda, M. Hamadam, T. Takeuchi, *J. Antibiot.* 29 (1976) 97;
(b) H. Umezawa, M. Ishizuka, T. Aoyagi, T. Takeuchi, *J. Antibiot.* 29 (1976) 857.
- [7] T. Osada, S. Ikegami, K. Takiguchi-Hayashi, Y. Yamazaki, Y. Katoh-Fukui, T. Higashinakagawa, Y. Sakaki, T. Takeuchi, *J. Neurosci.* 19 (1999) 6068.
- [8] A. Zaki, E.C. Schreiber, I. Weliky, J.R. Knill, J.A. Hubsher, *J. Clin. Pharmacol.* 14 (1974) 118.
- [9] J. Klastersky, D. Daneau, D. Weerts, *Chemotherapy* 18 (1973) 191.
- [10] J.R. Anaconda, *J. Coord. Chem.* 54 (2001) 355.
- [11] M.J. Lozano, J. Borrás, *J. Inorg. Biochem.* 31 (1987) 187.
- [12] A. Zhao, C.E. Carraher, G. Barone, C. Pellerito, M. Scopelliti, L. Pellerito, *Mater. Sci. Eng.* 93 (2005) 414.
- [13] M.S. Iqbal, A.R. Ahmad, M. Sabir, S.M. Asad, *J. Pharm. Pharmacol.* 51 (1999) 371.
- [14] J.R.J. Sorenson, *J. Med. Chem.* 19 (1976) 135.
- [15] D.H. Brown, W.E. Smith, J.W. Teape, A.J. Lewis, *J. Med. Chem.* 23 (1980) 729.
- [16] D.R. Williams, *The Metals of Life*, Van Nostrand Reinhold, London, 1971.
- [17] M. Ruiz, L. Perelló, R. Ortiz, A. Castiñeiras, C. Maichle-Mössmer, E. Cantón, *J. Inorg. Biochem.* 59 (1995) 801.
- [18] S.E. Castillo-Blum, N. Barba-Behrens, *Coord. Chem. Rev.* 196 (2000) 3.
- [19] I. Turel, I. Leban, N. Bukovec, *J. Inorg. Biochem.* 66 (1997) 241.
- [20] I. Turel, L. Goli, P. Bukovec, M. Gubina, *J. Inorg. Biochem.* 71 (1998) 53.
- [21] P. Yang, J.B. Li, Y.N. Tian, K.B. Yu, *Chin. Chem. Lett.* 10 (1999) 879.
- [22] G. Wu, G. Wang, X. Fu, L. Zhu, *Molecules* 8 (2) (2003) 287.
- [23] I. Turel, I. Leban, G. Klintschar, N. Bukovec, S. Zalar, *J. Inorg. Biochem.* 66 (1997) 77.
- [24] I. Turel, K. Gruber, I. Leban, N. Bukovec, *J. Inorg. Biochem.* 61 (1996) 197.
- [25] I. Turel, I. Leban, M. Zupancic, N. Bukovec, K. Gruber, *Acta Crystallogr. Sec C: Cryst. Struct. Commun.* 52 (1996) 2443.
- [26] Z.-F. Chen, R.-G. Xiong, J.-L. Zuo, Z. Guo, X.-Z. You, H.-K. Fun, *J. Chem. Soc. Dalton Trans.* (2000) 4013.
- [27] J. Al-Mustafa, *Acta Chim. Slov.* 49 (2002) 457.
- [28] M. Ruiz, L. Perelló, J. Server-Carrió, R. Ortiz, S. García-Granda, M.R. Díaz, E. Cantón, *J. Inorg. Biochem.* 69 (1998) 231.
- [29] M.S. Refat, *Synth. React. Inorg. Metal – Org. Chem.* 34 (9) (2004) 1605.
- [30] S.M. Teleb, M.S. Refat, *Bull. Chem. Tech. Maced.* 25 (1) (2006) 57.
- [31] Yu Ya Kharitonov, K.S. Sulaimankulov, N.B. Khudaibergenova, *Zh. Neorg. Khim.* 35 (8) (1990) 2117.
- [32] C.V. Deshpande, V.R. Rao, *J. Ind. Inst. Sci.* 69 (5) (1989) 329.
- [33] P.V. Vaidya, V.D. Deshpande, R. Rao, *J. Ind. Council Chem.* 3 (1) (1987) 21.
- [34] M.A. Tushchenko, V.B. Rybalka, A.I. Markina, A.A. Kostyuk, A.S. Tsitko, E.T. Denisenko, *Organ. Reagenty Anal. Khimii, Perm. Gos. Un-t, Perm* (1991) 43–38. (From: *Ref. Zh., Khim.* 1992, *Chem. Abstr.* No. 121:93018).
- [35] A.W. Bauer, W.M. Kirby, C. Sherris, M. Turck, *Am. J. Clin. Pathol.* 45 (1966) 493.
- [36] M.A. Pfaller, L. Burmeister, M.A. Bartlett, M.G. Rinaldi, *J. Clin. Microbiol.* 26 (1988) 1437.
- [37] National Committee for Clinical Laboratory Standards, *Performance Vol. Antimicrobial Susceptibility of Flavobacteria*, 1997.
- [38] National Committee for Clinical Laboratory Standards, *Methods for Dilution Antimicrobial Susceptibility Tests for Bacteria that Grow Aerobically*. Approved Standard M7-A3. National Committee for Clinical Laboratory Standards, Villanova, Pa, 1993.
- [39] National Committee for Clinical Laboratory Standards, *Reference Method for Broth Dilution Antifungal Susceptibility Testing of Conidium-Forming Filamentous Fungi: Proposed Standard M38-A*, NCCLS, Wayne, PA, USA, 2002.
- [40] National Committee for Clinical Laboratory Standards, *Methods for Antifungal Disk Diffusion Susceptibility Testing of Yeast: Proposed Guideline M44-P*. NCCLS, Wayne, PA, USA, 2003.
- [41] L.D. Liebowitz, H.R. Ashbee, E.G.V. Evans, Y. Chong, N. Mallatova, M. Zaidi, D. Gibbs, *Diagn. Microbiol. Infect. Dis.* 4 (2001) 27 (and Global Antifungal Surveillance Group).
- [42] M.J. Matar, L. Ostrosky-Zeichner, V.L. Paetznick, J.R. Rodriguez, E. Chen, J.H. Rex, *Antimicrob. Agents Chemother.* 47 (2003) 1647.
- [43] W.J. Geary, *Coord. Chem. Rev.* 7 (1971) 81.
- [44] I. Turel, L. Golic, O.L.R. Ramirez, *Acta Chem. Slov.* 46 (2) (1999) 203.
- [45] G.B. Deacon, R.J. Phillips, *Coord. Chem. Rev.* 33 (1980) 227.
- [46] A.W. Coats, J.P. Redfern, *Nature* 201 (1964) 68.
- [47] H.W. Horowitz, G.A. Metzger, *Anal. Chem.* 35 (1963) 1464.
- [48] N.K. Tunalı, S. Ozkar, *Inorg. Chem.*, Hazi University Publication, Ankara, Turkey, 1993, Pub. No. 185.
- [49] H. Arslan, U. Florke, N. Kulcu, M.F. Emen, *J. Coord. Chem.* 59 (2) (2006) 223.
- [50] A.A. Frost, R.G. Pearson, *Kinetics and Mechanism*, Wiley, New York, NY, USA, 1961.
- [51] C.X. Quan, L.H. Bin, G.G. Bang, *Mater. Chem. Phys.* 91 (2005) 317.
- [52] S.D. Cox, C.M. Mann, J.L. Markham, J.E. Gustafson, J.R. Warmington, S.G. Wyllie, *Molecules* 6 (2001) 87.